Transmission of a Two-Layer Coastal Kelvin Wave over a Ridge

PETER D. KILLWORTH

Deacon Laboratory of the Institute of Oceanographic Sciences, Wormley, Godalming, Surrey

(Manuscript received 10 October 1988, in final form 29 March 1989)

ABSTRACT

We consider the problem of a low-frequency, two-layer, coastal Kelvin wave which impinges on a topographic ridge or valley at some angle to the coastline, with the aim of bounding the transmission of the Kelvin wave beyond the topography (or, put alternatively, of bounding the scattering of energy into topographic waves along the ridge). The width of the topographic feature is assumed to be of order the internal deformation radius. It is not necessary to solve the very complicated interaction problem near the junction of the ridge and the coastline. Instead, a simple series of eigenvalue o.d.e.'s must be solved.

The main contribution to loss of energy by the Kelvin wave comes from long waves along the ridge. Whether this loss is significant depends crucially on whether the topography is high enough to intersect a density surface (in this case, the interface between the two layers). If the topography remains solely in the lower layer, then the Kelvin wave continues with negligible loss of energy in the limit of very small frequency.

In a continuously stratified fluid, topography of any height would cut through an infinite number of density strata, so that a more realistic model would permit the topography to intersect the interface. This case is also considered, and results in a finite loss of energy from the Kelvin wave to topographic waves along the ridge (as in the one-layer reduced gravity case considered in an earlier paper). As a rough guide, the amplitude of the transmitted wave is reduced by an amount approximately equal to the fractional depth of the fluid blocked by the topography. Thus, models that do not permit topography to break through a density interface give qualitatively different answers from those which do—which should be considered when second-generation ocean models are being constructed.

It is found that, even using a supercomputer, available numerical resolution cannot adequately represent the topographically trapped waves, so topographical scattering processes will inevitably be badly misrepresented in numerical models. The case of a continuously stratified fluid is also briefly considered, although solutions would be considerably more complicated to produce.

1. Introduction

Probably the least well-understood feature of ocean circulation is its interaction with the ocean floor. Numerical general circulation models handle topography rather crudely to date (the popular quasi-geostrophic models do not even permit any large variation in bottom depth). It is becoming clear that topography, and associated form drag, must play a fundamental role in the momentum balance of the Antarctic Circumpolar Current (cf. Johnson and Bryden 1988, for example). Yet the number of studies of topographic effects remains quite small, even given the experience of atmospheric modelers. The difficulties are well known. The simplest problem involving rotating, stratified flow and topographic interactions rapidly becomes too complicated for analytical methods, and recourse must be taken to numerical solutions.

A previous paper (Killworth 1988, hereafter I) sought to bridge this gap by posing a problem whose analytic difficulties could be by-passed provided one was prepared to accept bounds on a solution, rather than the solution itself. Fortunately, in most geophysical situations, this is quite acceptable, since our stock of exact analytic solutions seldom fits observed geometries or situations particularly well.

The problem considered was that of a single (low) frequency coastal Kelvin wave in a one-layer reduced-gravity model, which impinges on a topographic feature at some angle to the coastline. Because the frequency of oscillation is low, wave motions can exist only within a few deformation radii of the coastline or topography. It was assumed that the feature does not vary in cross section normal to some direction extending away from the coastline. Typically one would consider a ridge at right angles to the coastline, for example. It was shown how application of (approximate) mass and (exact) energy conservation to an area around the intersection of the coast and topography gave two equations in an infinite number of unknowns. One of the unknowns was the amplitude of the transmitted Kelvin wave; the others were the amplitudes of the long topographic waves on the ridge. Calculus of variations then yielded a minimum and a maximum amplitude of the transmitted wave, without solving the complicated inter-

Corresponding author address: Dr. Peter D. Killworth, Hooke Institute for Atmospheric Research, Clarendon Laboratory, Parks Road, Oxford OX1 3PU, United Kingdom.

action problem. Johnson (1989) has used a representation of topography as a collection of horizontal strips to give another method for attacking the problem.

The physics of that problem were restricted to permit simple solutions. The purpose of this paper is to lift two of those restrictions. First, we include more wave modes by having more than one active layer of fluid (cf. Willmott 1984). This allows rigid-lid barotropic motions, whose natural length scales (formally infinite) are much larger than the deformation radius scale relevant to Kelvin and topographic waves. The second modification is more fundamental. In a continuously stratified ocean, even very small topographic features cut through an infinite number of density strata, and thus block flows confined to those lower strata. (The difficulty of handling layers of zero depth has long been a stumbling block in the development of isopycnal models and actively dynamical layered models.) We now permit the ridge to be sufficiently high that it intersects the interface between the two layers. This blocks the lower layer flow quite efficiently, so that information can be transmitted between the separated sections of the lower layer, across the blocking topography, only via pressure gradients in the upper layer. (One could formally consider a trough, but there would be difficulties in deciding whether a third, denser, layer should be positioned in the trough. The analysis in this paper shows that a trough entirely occupied by lower layer fluid would permit total transmission of the wave in the limit of small frequency. Henceforth, ridges only are considered.)

It will be shown that whether or not the topography intersects the interface has a fundamental effect on the transmission of Kelvin wave energy. If the topography is confined to the lower layer, then in the limit of vanishingly small frequency, all of the Kelvin wave energy crosses the topography. However, if the topography intrudes into the upper layer, then a situation similar to the one-layer case occurs, in which a finite amount of energy (straightforwardly computed) is always scattered to the topography.

A brief discussion of the continuously stratified case is given, together with the effects of the grid resolution in numerical models.

2. The problem and governing equations

We consider a problem similar to that of I, sketched in side and plan views in Fig. 1. Two immiscible layers of fluid, of densities ρ_1, ρ_2, lie between a bottom, whose height above some reference depth is $D(x, y)$, and a rigid lid at the surface. We shall mainly consider cases where D is a function of x only, but the analysis is identical in other cases provided that contours of D are parallel to each other. The rigid lid is a design choice, to avoid including both baroclinic and barotropic deformation radii in the analysis; essentially the barotropic deformation radius is infinite. The topography may or may not intersect the interface between layers.

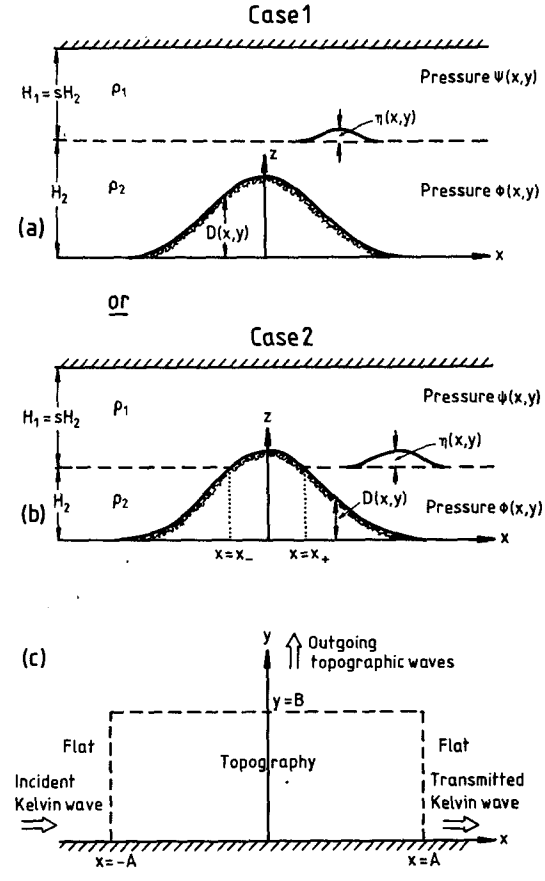

FIG. 1. Schematic of the problem, from the side (a, b) and in plan view (c). The ridge may be at any angle to the coastline, but is shown normal for simplicity. Two problems are considered. In the first, Case 1, the topography is confined to the lower layer. In the second, Case 2, there is a region in which the topography fills the lower layer and protrudes into the upper layer.

The undisturbed depths of the upper and lower layers are $H_1 = sH$ and $H_2 = H$, respectively, where s is the depth ratio. Pressures in the upper and lower layer are denoted by ψ, ϕ, respectively. The interface elevation is η. Horizontal velocities in layer i ($i = 1, 2$) are (u_i, v_i).

Two possible cases are considered: in case 1, the topography is nowhere high enough to break through the interface between layers; in case 2, there is a region in which the topography does break through the interface.

The area is confined by a rigid wall, or coastline, at $y = 0$. The topography D is assumed to be flat more than a few deformation radii away from $x = 0$, the axis of the topography. Far to the west ($x \to -\infty$), there is a monochromatic coastal Kelvin wave, of frequency ω, propagating to the east along the coastline. (It will be shown below that there is just one such wave.) This wave impinges on the topography, and scatters some of its energy as topographic waves. The remainder is

transmitted as a similar Kelvin wave, but with a change of both amplitude and phase. The problem is to bound the amplitude of the outgoing (transmitted) wave.

We first nondimensionalize the problem. A natural horizontal length scale is the deformation radius

$$a = \{g'Hs/f^2(s+1)\}^{1/2} \tag{2.1}$$

where g' is the reduced gravity $g(\rho_2 - \rho_1)/\rho_2$, and f is the Coriolis parameter, assumed constant over the region of interaction. Lengths are nondimensionalized on a, velocities on af, (pressures/density) and $g'\eta$ on $(af)^2$, frequency ω on f, and topographic height D on H. We assume that all quantities vary with time t as $\exp(-i\omega t)$. As in I, it will be assumed that

$$\omega \ll 1, \tag{2.2}$$

i.e., that the wave frequency is low.

The momentum equations then become

$$-i\omega u_1 - v_1 = -\psi_x \tag{2.3}$$

$$-i\omega v_1 + u_1 = -\psi_y \tag{2.4}$$

$$-i\omega u_2 - v_2 = -\phi_x \tag{2.5}$$

$$-i\omega v_2 + u_2 = -\phi_y. \tag{2.6}$$

The hydrostatic relation links the upper and lower layer pressures through the interface elevation η:

$$\psi = \phi - \eta \tag{2.7}$$

in regions of the fluid where there are two active fluid layers (elsewhere ϕ, η are undefined).

The divergence equations depend on the number of active layers. When layers 1 and 2 both exist, (case 1, and part of case 2)

$$i\omega\eta + (1+s)\nabla\cdot\mathbf{u}_1 = 0 \tag{2.8}$$

$$-i\omega\eta + \{(1+s)/s\}\nabla\cdot\{(1-D)\mathbf{u}_2\} = 0 \tag{2.9}$$

whereas when only layer 1 exists (in some areas of case 2)

$$\nabla\cdot\{(s-D+1)\mathbf{u}_1\} = 0. \tag{2.10}$$

These equations can be combined. We first solve for u_i, v_i in terms of the pressures, to leading order in ω:

$$v_1 = \psi_x + i\omega\psi_y, \quad u_1 = -\psi_y + i\omega\psi_x \tag{2.11}$$

$$v_2 = \phi_x + i\omega\phi_y, \quad u_2 = -\phi_y + i\omega\phi_x \tag{2.12}$$

and substitute in the divergence equations. When there are two layers, this gives

$$\eta + (1+s)\nabla^2\psi = 0 \tag{2.13}$$

$$(1-D)\nabla^2\phi - s\eta/(s+1) + iD_x(-\phi_y + i\omega\phi_x)/\omega = 0 \tag{2.14}$$

where we have assumed $D = D(x)$ only for simplicity. When there is one active layer only, we have

$$(s-D+1)\nabla^2\psi + iD_x(-\psi_y + i\omega\psi_x)/\omega = 0. \tag{2.15}$$

The system (2.13) to (2.15) needs boundary and (for case 2) jump conditions. In case 2, we assume that the depth of the lower layer vanishes (i.e., $D = H = 1$, nondimensionally) at values of $x = x_-, x_+$. Then in the upper layer, (2.15) shows that both mass and tangential velocity must be continuous at $x = x_-, x_+$. The requirement that the bottom layer be well behaved means that velocities remain finite there. This gives the conditions

$$\psi, \psi_x \text{ are continuous, and } (1-D)\phi_x = 0, \quad x = x_-, x_+. \tag{2.16}$$

At the boundary $y = 0$, there is no normal velocity

$$v_1 = v_2 = 0, \quad y = 0. \tag{2.17}$$

We require only waves with positive group velocity northwards as $y \to \infty$ (i.e., there be no waves approaching from $+\infty$). Finally, when $|x|$ becomes large, there can only be a Kelvin wave, which is confined to the near-coastal region.

The solution for the Kelvin wave is straightforward. To leading order we find

$$x \to -\infty: \quad \{\eta, \phi, \psi\} = \{1, s/(s+1), -1/(s+1)\}\exp(i\omega x - y) \tag{2.18}$$

$$x \to +\infty: \quad \{\eta, \phi, \psi\} = \eta_T\{1, s/(s+1), -1/(s+1)\}\exp(i\omega x - y) \tag{2.19}$$

where η_T is the unknown amplitude (and phase) of the transmitted Kelvin wave. As noted above, there are barotropic motions with length scales much longer than unity (the deformation radius), but such motions are restricted by the rigid-lid assumption to being nondivergent and hence cannot occur along the coast as a wave. A free surface would permit a barotropic Kelvin wave with a decay scale of the barotropic deformation radius; over the length scales considered here such a wave would be independent of position, and therefore play no role.

3. The case of no topographic breakthrough: Mass/energy conservation

Consider first case 1, in which the topography remains confined to the lower layer. We proceed, formally, as in I. First, integrate either of the mass continuity equations across the region indicated in Fig. 1. The region is bounded by $x = \pm A$, for some A of order unity, and $y = B$, where B is also of order unity. The rationale for the choice of A and B needs a little care. As in I, A and B must be sufficiently large so that the baroclinic wave fields associated with the topography have decayed away, and yet not so large so that the area $2AB$ becomes of order ω^{-1}, which invalidates the mass conservation argument to be given below. There are other difficulties, because the barotropic component of the pressure fields decays very slowly (as

$\exp(-\omega|x|)$, for example). However, this gives only a negligible contribution to the velocity fields being integrated, as we shall see.

Integrating (2.9), then, gives

$$\left[\int_0^B u_2 dy\right]_{-A}^{A} + \int (1-D)v_{2B}dx = O(\omega) \ll 1 \quad (3.1)$$

under these conditions, where the subscript B denotes evaluation at $y = B$. Henceforth, integrals wrt x without limits denote limits of $(-\infty, \infty)$ or $(-A, A)$, and will usually be obvious. Using (2.18) and (2.19), this can be rewritten

$$\{s/(s+1)\}(\eta_T - 1) + \int (1-D)v_{2B}dx = O(\omega) \ll 1. \quad (3.2)$$

and provides one constraint on the solution.

Energy conservation (which is exact) provides another. Adding $su_1^* \times (2.3)$, $sv_1^* \times (2.4)$, $s\psi/(1+s) \times (2.8)^*$, $(1-D)u_2^* \times (2.5)$, $(1-D)v_2^* \times (2.6)$, and $s\phi/(1+s) \times (2.9)^*$, where asterisks denote complex conjugate, gives

$$\nabla \cdot \{s\psi \mathbf{u}_1^* + (1-D)\phi \mathbf{u}_2^*\} = \text{pure imaginary} \quad (3.3)$$

so that integration gives

$$\left[\int_0^B \{s\psi u_1^* + (1-D)\phi u_2^*\}dy\right]_{-A}^{A} + \int \{s\psi_B v_{1B}^* + (1-D)\phi v_{2B}^*\}dx = \text{pure imaginary}. \quad (3.4)$$

Use of the Kelvin wave conditions simplifies this to

$$\{s/[2(s+1)]\}\{|\eta_T|^2 - 1\} + \text{Re}\int \{s\psi_B v_{1B}^* + (1-D)\phi v_{2B}^*\}dx = 0. \quad (3.5)$$

Thus we have two conditions (3.2), (3.5), on the transmitted coefficient η_T.

Note finally that integration of the depth weighted sum of the two mass continuity equations yields conservation of the barotropic flow:

$$\left[\int_0^B (su_1 + u_2)dy\right]_{-A}^{A} + \int (sv_{1B} + (1-D)v_{2B})dx = O(\omega) \ll 1 \quad (3.6)$$

and since the inflows and outflows balance baroclinically,

$$\int (sv_{1B} + (1-D)v_{2B})dx = O(\omega) \ll 1 \quad (3.7)$$

a condition which will be used to advantage later.

4. The case of no topographic breakthrough: Topographic waves

To proceed, it is necessary to understand the properties of waves confined by topography. Many features of these have been known for some time; see the review by Mysak (1980), or Huthnance (1978), for example. We pose a wave varying along the topography as $\exp(ily)$, where l is an (unknown) wavenumber. Choosing to describe the wave by the lower layer pressure ϕ and the interface elevation η, we put

$$\eta = G(x)\exp(ily), \quad \phi = F(x)\exp(ily). \quad (4.1)$$

Substituting into (2.13), (2.14) yields the governing equations

$$(1+s)(F'' - G'') = l^2(1+s)(F-G) - G \quad (4.2)$$

$$[(1-D)F']' = [l^2(1-D) - lD'/\omega]F + sG/(s+1) \quad (4.3)$$

where a prime denotes differentiation wrt x. These eigenvalue equations are to be solved subject to the boundary condition that F, G vanish as $|x| \to \infty$. We note that, for large enough $|x|$, D is infinitesimally small, so that (4.2), (4.3) have the asymptotic solutions

$$B \to G_0 \exp(-|x|(1+l^2)^{1/2}) \quad (4.4)$$

$$F \to F_0 \exp(-l|x|) + sG/(s+1), \quad |x| \to \infty. \quad (4.5)$$

Here F_0, G_0 are some unknown constants. The form of these asymptotic solutions is quite important. Here G decays on a scale at least as fast as the deformation radius (unity), as befits a baroclinic field. However, F also possesses a barotropic component, and thus decays like a simple solution of Laplace's equation. When l is small, this decay rate is very slow. [However, the u field generated by this is also very small, of order ω, and so generates a negligible change to the balance (3.2).]

The system [(4.2), (4.3)] has three kinds of solutions. The first two are familiar from I, while the third owes its existence to the finite depth now permitted.

Long waves exist, for which

$$l = l_0\omega, \quad \text{for some } l_0 \text{ of order unity.} \quad (4.6)$$

Substituting, we have

$$F'' - G'' = -G/(1+s) \quad (4.7)$$

$$[(1-D)F']' = -l_0 D'F + sG/(s+1) \quad (4.8)$$

so that

$$G' = \mp G, \quad F' \pm \omega l_0 F = \{s/(s+1)\}(G' \pm \omega l_0 G), \quad x \to \pm\infty. \quad (4.9)$$

This gives a countable collection of long-wave modes, a finite number of which occur for any finite frequency ω. Unlike I, however, there is, in addition to the com-

ponent which decays at least as fast as the deformation radius, a component which decays slowly with x, as $\exp(-\omega|x|)$; this will have important consequences.

Short waves exist, for which

$$l = l_2/\omega, \quad \text{for some } l_2 \text{ of order unity.} \quad (4.10)$$

Substituting,

$$F = G \quad (4.11)$$

$$[(1 - D)F']' = [l_2^2(1 - D) - l_2 D']F/\omega^2 \quad (4.12)$$

so that there is zero pressure ($F - G$) in the upper layer (motion is thus confined to the lower layer), and the lower-layer equation (4.12) is identical to the similar case for a single layer in I. There, it was shown that the short waves are confined within a width of order $\omega^{1/2}$ to a specific x value, with rapid x-oscillations on a scale of order ω.

A single additional mode, here termed *quasi-barotropic* (or QB), can occur. This is a very long mode, with

$$l = l_1\omega^2, \quad \text{for some } l_1 \text{ of order unity.} \quad (4.13)$$

Solutions are found with

$$F = 1 + \omega F_1 + \omega^2 F_2 + \cdots$$

$$G = \omega G_1 + \omega^2 G_2 + \cdots. \quad (4.14)$$

The $O(\omega)$ terms give, after a little algebra,

$$(1 + s)(F_1'' - G_1'') = -G_1$$

$$(s + 1 - D)F_1' - sG_1' = -l_1 D. \quad (4.15)$$

These combine to give a second-order d.e. for G_1, which, together with the easily derived condition $G \to 0$, $|x| \to \infty$, determines the eigenvalue l_1. Because F is constant to leading order, the mode varies only slowly in both x and y [and thus contributes only a very tiny amount to the (u, v) field]. As $s \to \infty$, this mode tends smoothly to the first one-layer mode (cf. I). As the wavenumber of the QB mode increases, so that the mode is no longer very long, the behavior resembles the other modes.

Figure 2a gives a typical, numerically evaluated, dispersion diagram for the case $s = 10$, and

$$D = 0.5 \operatorname{sech}^2(x/2). \quad (4.16)$$

corresponding to a smooth ridge centered on $x = 0$. (The large value of s was chosen to simulate a thin layer of fluid at the ocean bottom, but all values of s give similar structures, throughout this paper.) The first mode is the ultralong QB mode discussed above; the others shown are all long. If one follows a given mode as l increases, the mode may be considered long until the maximum frequency has been achieved, and is then short. The curve is little different from Fig. 2 in I, which can be thought of as the limit $s \to \infty$. The only (mathematical) difference is that for the QB mode, l varies as ω^2 for very small ω, rather than the long-wave limit

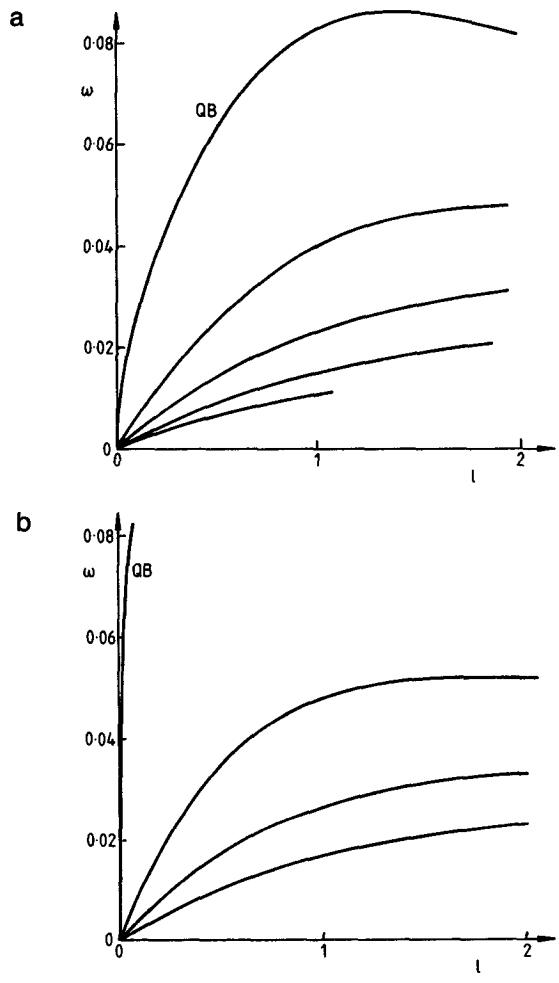

FIG. 2. (a) The dispersion relation for topography (4.16), and $s = 10$. There is a second set of modes with wavenumber l replaced by $-l$. The QB mode is indicated. Short waves are arduous to find numerically, since very fine accuracy and resolution are needed, and so are not shown. (b) As in (a), but with $s = 1$.

of $O(\omega)$ in I. The curves have the same qualitative character for wide variations of the parameters; cf. Fig. 2b, when the upper-layer depth s is only 1.

Figure 3a shows the spatial structure of some of the modes in Fig. 2a. When s is large (10 in the example), (4.2) shows that $P \equiv (F - G)$ is small, of order $(1/s)$, except when l is very small. Thus, the QB mode [Fig. 3a(i)] has a varying upper layer pressure, but the higher modes [Figs. 3a(ii), (iii)] have very small surface pressure, and are very similar to the case considered in I. When s is of order 1 (Fig. 3b), then apart from the QB mode (for which the interface height is very small, and the pressure essentially barotropic), the modes all involve interaction between the two layers.

5. The case of no topographic breakthrough: The transmission

We now demonstrate that the transmission, $|\eta_T|$, for sufficiently small frequency, is 100%. Two methods

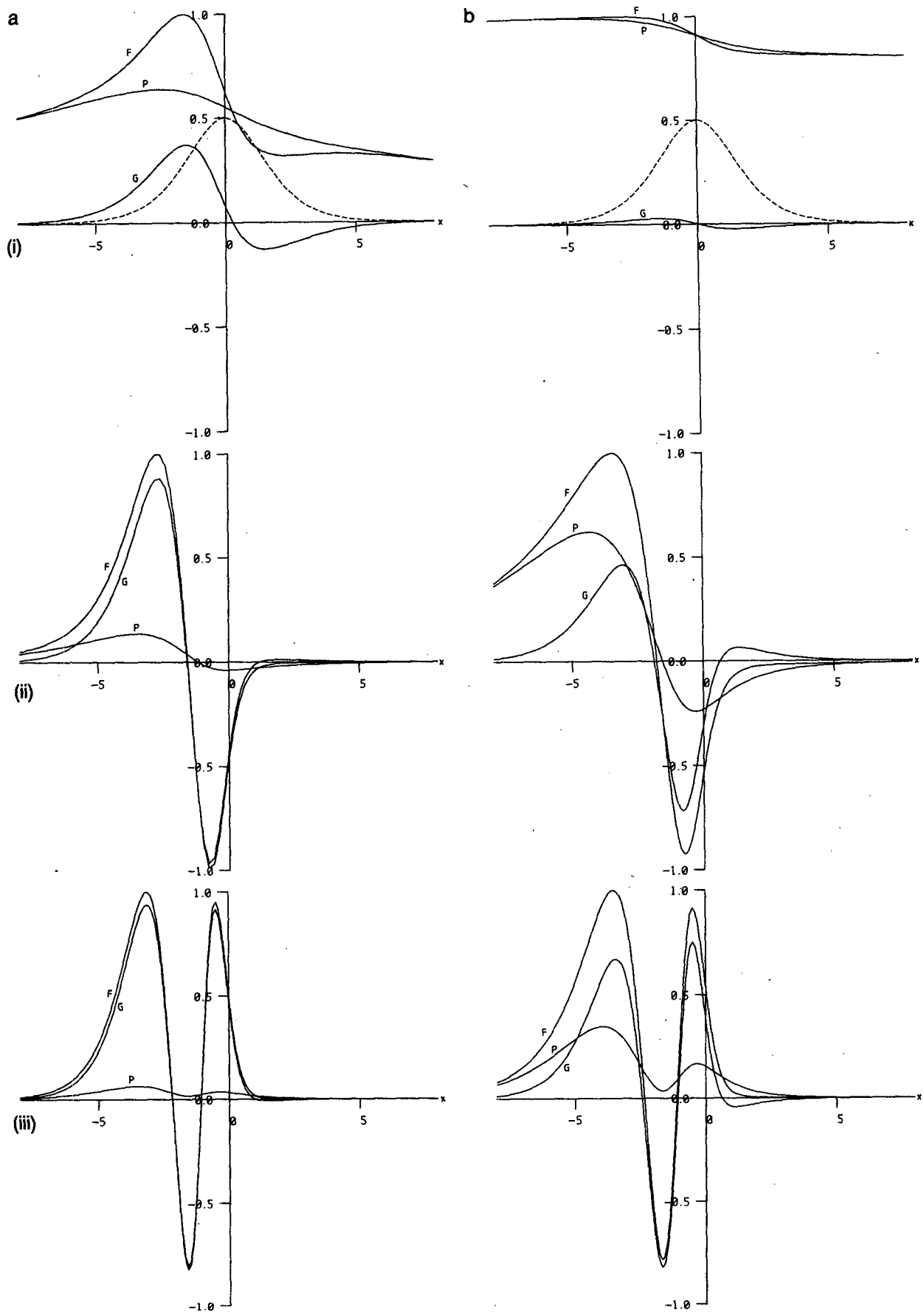
a
b
(i)
(ii)
(iii)
F
P
G
1.0
0.5
0.0
-0.5
-1.0
-5
0
5
x

will be used. The first is not totally rigorous, but demonstrates physically why this is the case. The second, rather longer, is a fuller mathematical treatment.

We write the solution at $y = B$ in terms of topographic waves

$$\eta = \sum \alpha_n G_n(x) \exp(il_n B) \tag{5.1}$$

$$\phi = \sum \alpha_n F_n(x) \exp(il_n B) \tag{5.2}$$

the sums being taken over the mode number n for the waves. The unknown coefficients α_n are assumed O(1) for the simple derivation.

Substituting into mass and energy conservation (3.2), (3.5), and neglecting terms of order ω, we have

$$\{s/(s+1)\}(\eta_T - 1) + \sum \alpha_n \exp(il_n B) \times \int (1-D)(F'_n - \omega l_n F_n)dx = 0 \tag{5.3}$$

$$\{s/[2(s+1)]\}(|\eta_T|^2 - 1) + \sum |\alpha_n|^2 \times \int dx[s(F_n - G_n)\{F'_n - G'_n - \omega l_n(F_n - G_n)\} + (1-D)F_n(F'_n - \omega l_n F_n)] + \sum_{m<n} Q_{mn} \times \int dx\{R_{mn} + R_{nm}\} = 0 \tag{5.4}$$

where

$$Q_{mn} = \mathrm{Re}(\alpha_m \alpha_n^*) \exp i(l_m - l_n)y \tag{5.5a}$$

$$R_{mn} = s(F_m - G_m)[F'_n - G'_n - \omega l_n(F_n - G_n)] + (1-D)F_m(F'_n - G'_n). \tag{5.5b}$$

Note that the x-integrals will eventually be taken over the range $(-\infty, +\infty)$, rather than $(-A, A)$. The justification is as follows. In the mass continuity equation (5.3), the first term in the integral can be integrated by parts to yield

$$\int_{-A}^{A} D'F_n dx \tag{5.6}$$

plus contributions at $\pm A$. If A is large enough for D' to be negligible there, these can be ignored. Then the integral in (5.6) can be taken over an infinite range with no loss of accuracy. The second term's contribution, outside $\pm A$, is at most of order ω from (4.5); terms of that order have already been neglected in deriving (5.3). Hence the conversion from finite to infinite limits in (5.3) is legitimate. Virtually identical reasoning holds for (5.4) also.

The simple argument is straightforward. We need merely show that the integrals multiplying the α_n in (5.3) are at most $O(\omega)$. Then we obtain the result

$$\eta_T = 1 - O(\omega). \tag{5.7}$$

To see this, apply (3.7)—which also applies to each wave mode—to write the integral in (5.3) in terms of the top layer pressure

$$\int (1-D)(F'_n - \omega l_n F_n)dx = -\int (P'_n - \omega l_n P_n)dx. \tag{5.8}$$

The first term vanishes by integration (because the upper-layer depth is uniform; the result will be very different for the breakthrough case), and the second, even taking the slow decay with x into account, is at most of order ω, for the QB and long modes, and far smaller for the short modes because of the limited x-extent involved. Thus (5.7) is proved, albeit nonrigorously. This approach gives no idea of the sizes of the various modal components, however; for that we need the rigorous approach.

First, we derive an orthogonality relationship. Multiply $(F_m - G_m)$ by (4.2, with wavenumber l_n), and add $F_m \times$ (4.3, with wavenumber l_n). From this subtract the same quantity with m and n interchanged. The result is integrated wrt x over the infinite range, and divided by $(l_n - l_m)$, assumed nonzero. The result is

$$\int dx[s(l_n + l_m)(F_n - G_n)(F_m - G_m) + (1-D)(l_n + l_m)F_n F_m - D'F_n F_m/\omega] = 0, \quad m \neq n. \tag{5.9}$$

Examination of the Q_{mn} term in (5.4) shows that this vanishes identically by (5.9) just derived. Thus, as in I, only the self-interaction quadratic terms survive in (5.4).

Next, we rewrite (5.3), (5.4) as

$$\eta_T - 1 + \{(s+1)/s\} \sum \alpha_n \gamma_n = 0 \quad \text{to leading order} \tag{5.10}$$

$$|\eta_T|^2 - 1 + \{(s+1)/s\} \sum |\alpha_n|^2 \mu_n \gamma_n = 0 \quad \text{to leading order} \tag{5.11}$$

where

$$\gamma_n = \exp(il_n B) \int (1-D)(F'_n - \omega l_n F_n)dx = \int (1-D)(F'_n - \omega l_n F_n)dx \quad \text{for all but short waves} \tag{5.12}$$

FIG. 3. (a) The spatial structure of the first three modes for topography (4.16), with $s = 10$ and $\omega = 0.02$. (i, ii, iii) show the QB mode and the first two long modes, respectively; (i) also shows the topography as a dashed line. The upper and lower layer pressures (P, F) and the interface elevation G are indicated. (b) As in (a) but for $s = 1$.

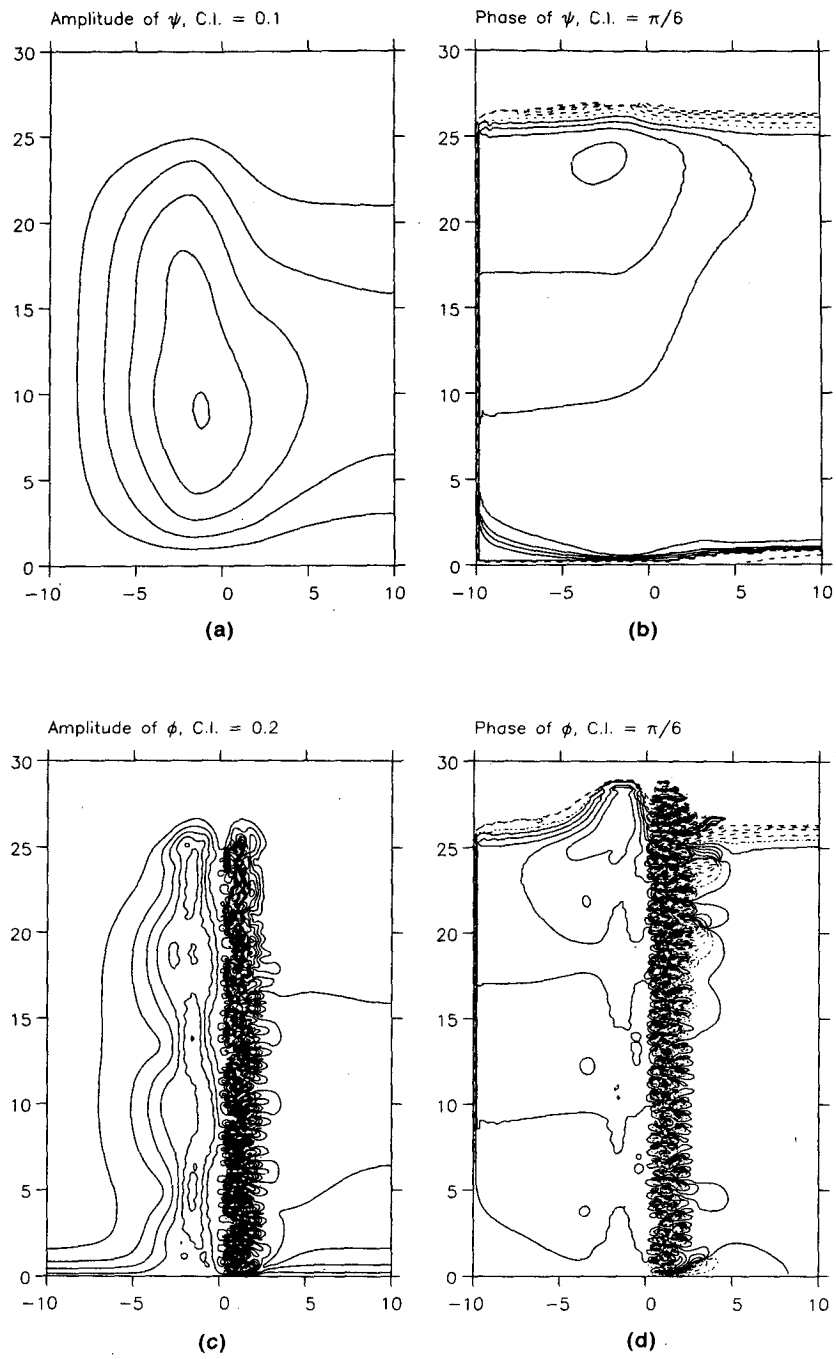

FIG. 4. The solution of (2.13), (2.14) for topography (4.16) and frequency 0.02, with the depth ratio $s = 10$. The modulus and phase of ψ are shown in (a), (b), respectively; the modulus and phase of ϕ in (c), (d); and the modulus and phase of η in (e), (f). Contours and cross section of topography are shown in (g), (h). Contour intervals shown above each diagram. A linear decay ("glue") has been inserted for $y > 25$ in order to remove reflection effects from the northern boundary. On the western boundary, an incoming Kelvin wave is specified; on the eastern side, a radiation condition is applied. The resolution is 100×400.

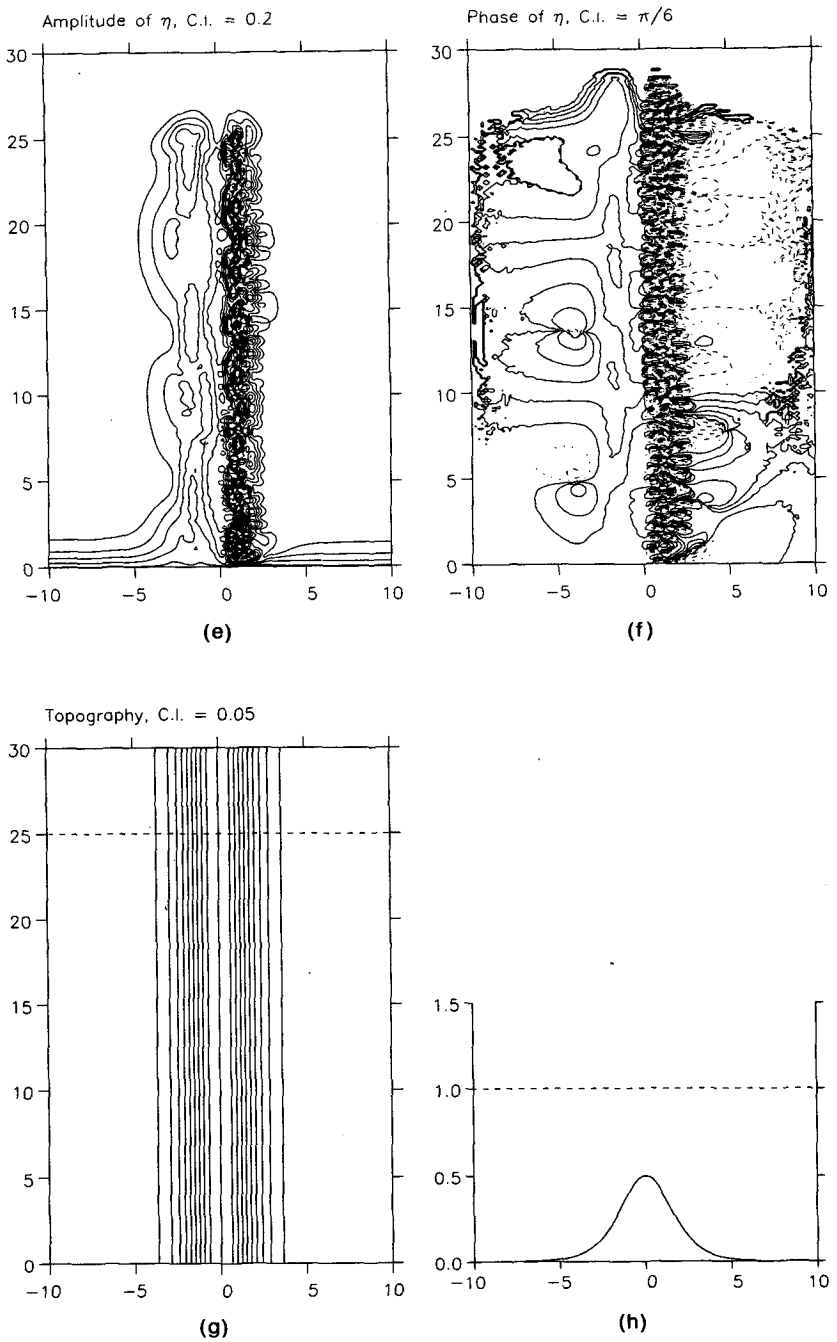

FIG. 4. (*Continued*)

(which are unimportant, as in I, since the l_n are small) and

$$\mu_n\gamma_n^2 = \int \{D'F_n^2 - 2\omega l_n[s(F_n - G_n)^2 + (1 - D)F_n^2]\}\,dx$$

$$= \int D'F_n^2\,dx + O(\omega) \qquad (5.13)$$

as in I again. The quantities γ_n, μ_n are readily computed from (4.2), (4.3) as a simple eigenvalue problem.

Now (5.10), (5.11) possess entirely the same structure as in section 4 of I, save for the $(s + 1)/s$ factors. The entire extremum calculation for $|\eta_T|$ in I thus proceeds almost unchanged, and only the essential formulae will be quoted. Defining, as before,

$$\sigma = \sum \mu_n^{-1} \qquad (5.14)$$

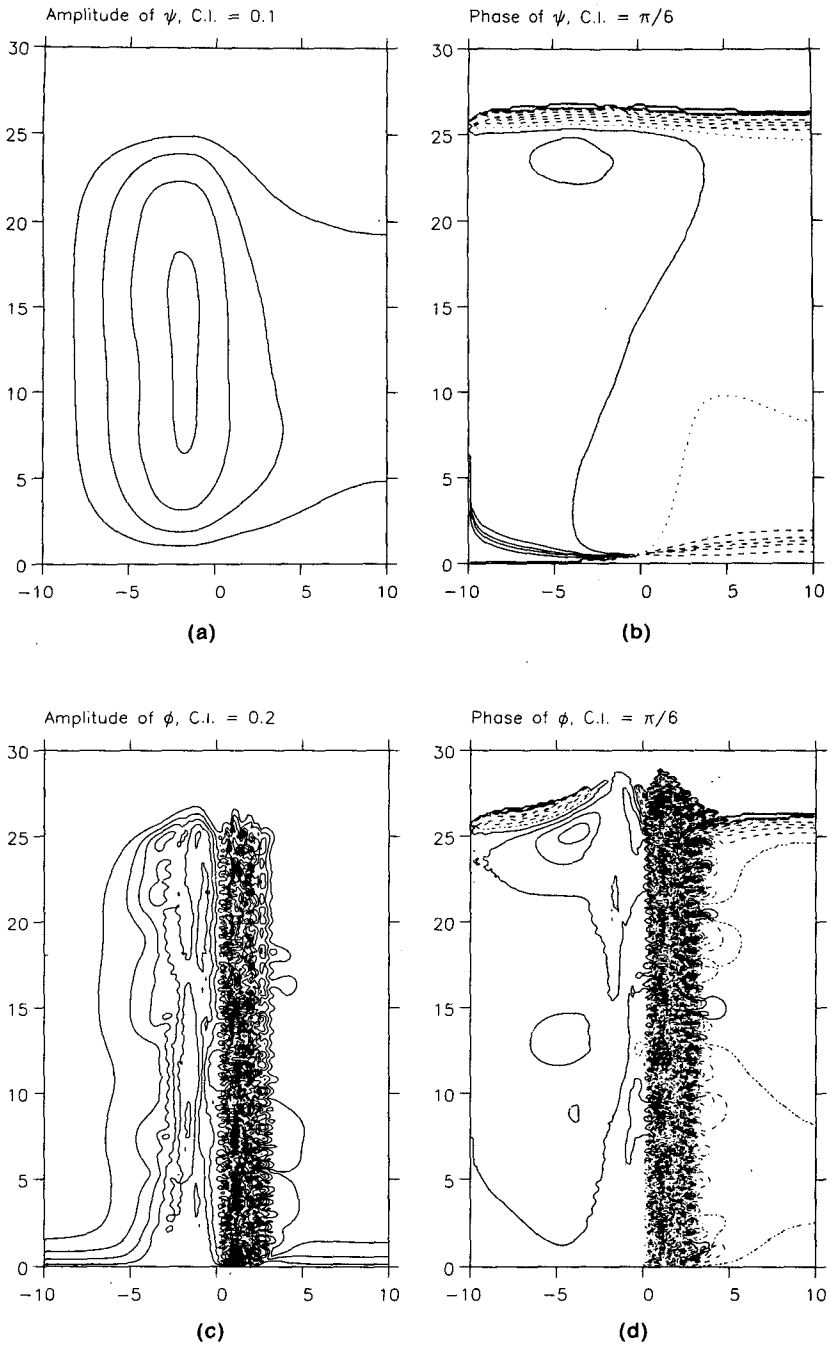

FIG. 5. as in Fig. 4a–f, but for $\omega = 0.01$.

we find

$$(1 - A\sigma)/(1 + A\sigma) \leqslant |\eta_T| \leqslant \{(1 - A\sigma)/(1 + A\sigma)\}^{1/2}. \quad (5.15)$$

Here

$$A = (s + 1)/s$$

has been defined.

The relative contributions of each mode to the integrals is simple to estimate; the arguments are omitted for brevity. We find that

$$\gamma_n \sim \begin{cases} O(\omega), & \text{QB mode} \\ O(\omega), & \text{long mode} \\ O(\omega^2), & \text{short mode} \end{cases}$$

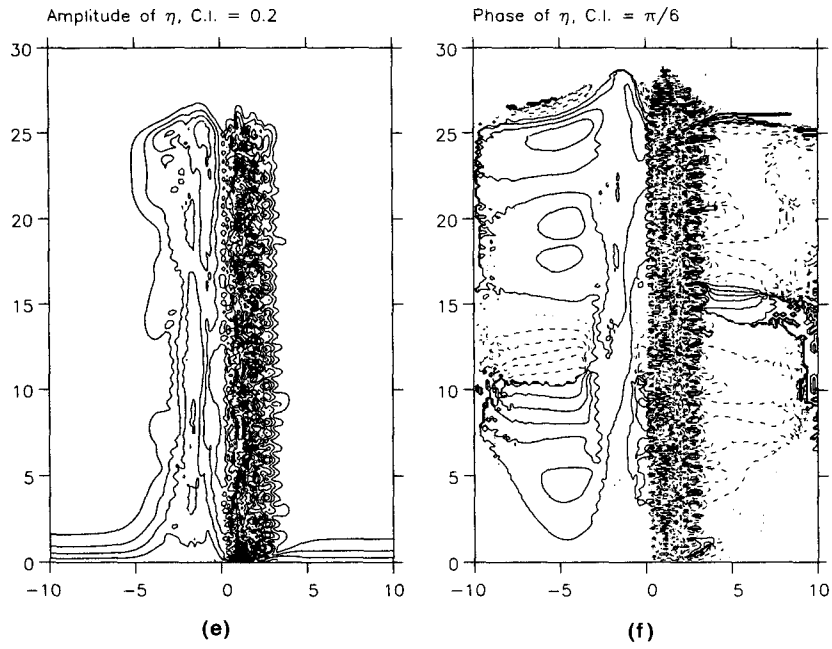

FIG. 5. (*Continued*)

while the integrals in (5.13) are

$$\begin{aligned} &O(\omega), && \text{QB mode} \\ &O(1), && \text{long mode} \\ &O(\omega^{1/2}), && \text{short mode} \end{aligned}$$

so that

$$\mu_n \sim \begin{cases} O(\omega^{-1}), & \text{QB mode} \\ O(\omega^{-2}), & \text{long mode} \\ \gg 1, & \text{short mode.} \end{cases}$$

Thus

$$\sigma = O(\omega)$$

from the QB contribution. Both minimization and maximization give values of the coefficients α_n of the same order. It is found that only the QB mode has a coefficient of order unity, with all long modes having a coefficient of order ω. (Note that the small energy loss, of order ω, is produced by both QB and long modes.) The velocities along the topography (and not near the coastline) are O(1), while the velocities parallel to the coastline remain small.

Figures 4 and 5 show two numerical examples, computed by direct solution of (2.13), (2.14) together with boundary conditions. The depth ratio s is 10, and the frequency ω is 0.02, 0.01, respectively. The behaviour predicted here is clearly visible, with long waves

TABLE 1. Comparison of numerical and analytical solutions, $s = 10$, $D_m = 0.5$.

	Transmission	
Frequency	Numerical	Analytical
0.02	0.76	$0.55 \leqslant \lvert\eta_T\rvert \leqslant 0.74$
0.01	0.83	$0.70 \leqslant \lvert\eta_T\rvert \leqslant 0.84$
0.005	not resolved	$0.85 \leqslant \lvert\eta_T\rvert \leqslant 0.92$

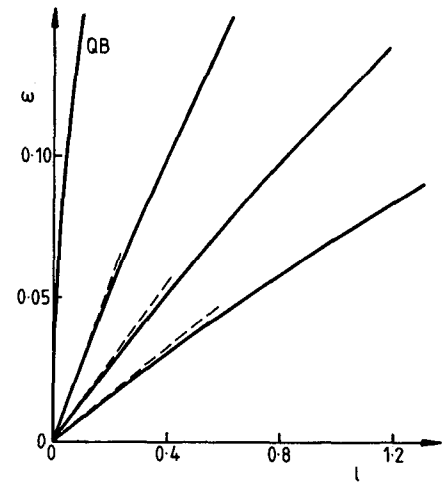

FIG. 6. Part of the dispersion relation for topography (7.10), $s = 5$. The topography breaks through into the upper layer for this case. The long wave limit (mentioned briefly in the text) is shown dashed. The QB mode is indicated.

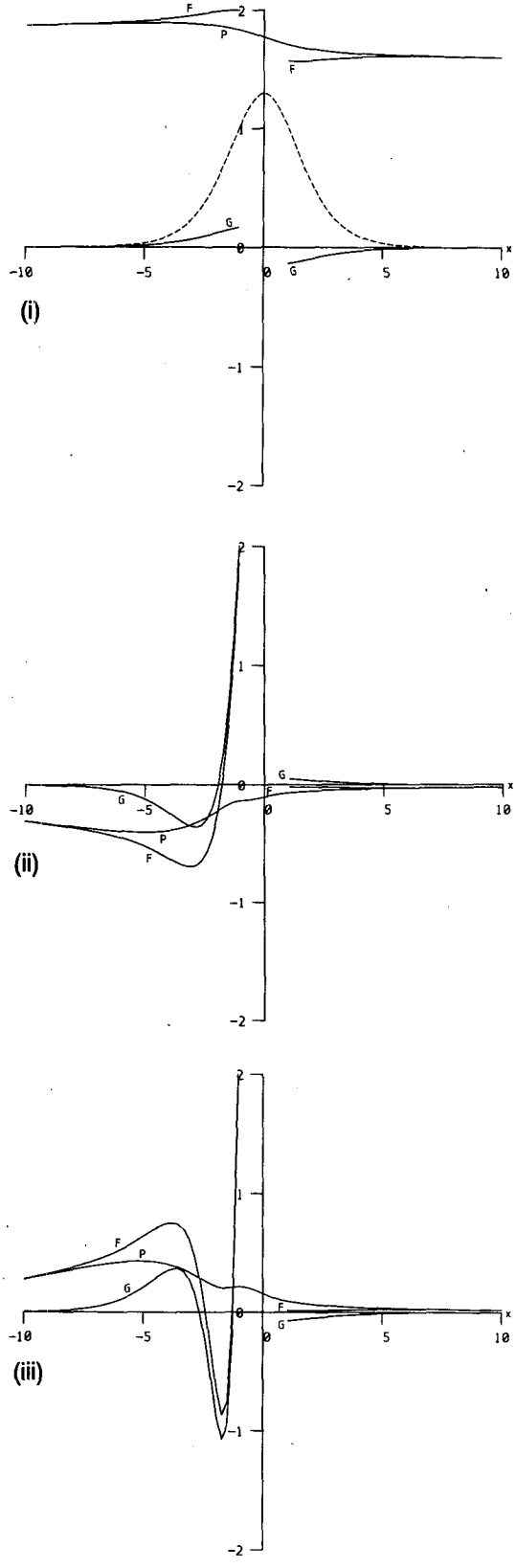

FIG. 7. The spatial structure of the QB and the first two long modes, for $\omega = 0.02$. Annotations as in Fig. 3.

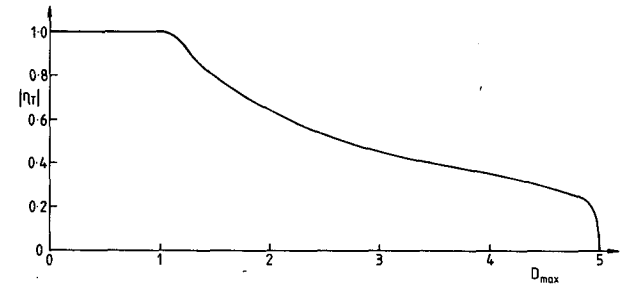

FIG. 8. The dependence of the amplitude of the transmitted wave $|\eta_T|$ with maximum topographic height D_{max}, for the long-wave solution (i.e., vanishingly small frequency), topography (7.10), and depth ratio $s = 5$. There is 100% transmission for D_{max} less than unity. Slight irregularities in the curve are due to cumulative rounding errors.

lengthening, and short waves shortening, as the frequency decreases. The structure of ψ is almost entirely governed by the QB mode, and a much wider numerical box would be needed to let ψ decay satisfactorily at large values of $|x|$. The transmissions are given in Table 1; it is unfortunate that numerical restrictions prevented the case $\omega = 0.005$ for comparison. As in I, note that the upper bound on $|\eta_T|$, which varies as in (5.7), is in excellent agreement with the computed transmission coefficient (although this agreement, while convenient, is of less immediate use than before).

Thus the situation for the case of no topographic breakthrough is simple; for small enough frequency, two-layer coastal Kelvin waves can pass across a partial topographic barrier with negligible loss of energy.

6. The case of topographic breakthrough: Mass/energy conservation

We now consider case 2, in which the topography is sufficiently high to outcrop into the surface layer in the region $x_- \leqslant x \leqslant x_+$. The governing equations remain unchanged. Define the operator

$$C[\lambda] = \left\{\int_{-\infty}^{x_-} + \int_{x_+}^{\infty}\right\}\lambda dx \qquad (6.1)$$

as the natural definition of an integral across the lower layer (the integral is well defined because all quantities are well behaved at $x = x_-, x_+$). Integration of mass continuity (2.9) then gives

$$\left[\int_0^B u_2 dy\right]_{-A}^{A} + C[(1 - D)v_{2B}] = O(\omega), \qquad (6.2)$$

i.e., using (2.18), (2.19)

$$\{s/(s + 1)\}(\eta_T - 1) + C[(1 - D)v_{2B}] = O(\omega). \qquad (6.3)$$

Note that the incoming lower layer flow must perforce turn and flow in the positive y-direction along the left flank of the topography, to conserve mass; the outgoing lower layer flow is similarly provided for by a net flow in the negative y-direction along the right flank of the topography. Integration of the upper-layer flow gives no more information (but provides useful checks on numerical evaluation of integrals). This is because the net barotropic flow away from the coast must be zero, by integrating the sum of (2.8) and (2.9):

$$\int (s - D_1)v_{1B}dx + C[(1 - D)v_{2B}] = 0 \quad (6.4)$$

a condition which will be used later.

The energy calculation is similar, yielding

$$\{s/2(s+1)\{[|\eta_T|^2 - 1] + \mathrm{Re}\left\{\int (s - D_1)\psi_B v_{1B}^* dx + C[(1 - D)\phi_B v_{2B}^*]\right\} = 0 \quad (6.5)$$

where D_1 is the amount of topography extending above the interface, defined to be zero for $D < 1$, and equal to $(D - 1)$ otherwise. Then eqns. (6.3), (6.4) provide two equations which enable bounds to be placed on $|\eta_T|$.

7. The case of topographic breakthrough: Topographic waves

We proceed as before, defining η and ϕ in terms of wave modes as in (4.1), together with the upper-layer pressure

$$\psi = P(x)\exp(ily). \quad (7.1)$$

Where there are two active layers, we have (4.2), (4.3) again:

$$(1 + s)P'' = l^2(1 + s)P - G \quad (7.2)$$

$$[(1 - D)F']' = [l^2(1 - D) - lD'/\omega]F + sG/(s + 1) \quad (7.3)$$

together with the definition

$$P = F - G. \quad (7.4)$$

When there is only one active layer,

$$[(s - D + 1)P']' = [l^2(s - D + 1) - lD'/\omega]P. \quad (7.5)$$

There are connection formulae

$$(1 - D)F' = 0; \quad P, P' \text{ continuous at } x = x_-, x_+ \quad (7.6)$$

and boundary conditions

$$F, G, P \to 0, \quad |x| \to \infty. \quad (7.7)$$

The appropriate asymptotic formulae are of course identical with (4.4), (4.5).

Again, there are three types of topographic wave mode: quasi-barotropic, long, and short. The relevant formulae for the size of the wavenumbers, etc., in section 4 continue to apply. The long waves (which will be relevant for what follows) trivially satisfy

$$l = l_0\omega. \quad (7.8)$$

Where there are two layers, (4.7), (4.8) hold, and where there is only one layer,

$$[(s - D + 1)P']' = -l_0 D'P. \quad (7.9)$$

Figure 6 shows the (lower part of) the numerically obtained dispersion relation for

$$s = 5, \quad D = D_{\max}\,\mathrm{sech}^2(x/2), \quad \text{where } D_{\max} = 1.3. \quad (7.10)$$

The cutoff frequency is much higher than the low frequencies shown in the diagram, so that the dispersion curves are close to straight lines. The dashed line shows the long wave limit, obtained from the above.

Figure 7 shows the spatial variation of the first three modes for $\omega = 0.02$ for this geometry. In all cases, the upper-layer pressure P varies smoothly with x. With increasing mode number, the lower-layer pressure F not only oscillates more—as with any modal set—but also the length scale over which F varies drops rapidly, especially near x_- (the numerical roughness is a feature of the plotting frequency, not of the numerical solution). This indicates that finite-difference general circulation models are likely to have resolution problems in such locations, even assuming that a satisfactory numerical scheme exists to handle vanishing layer depths.

8. The case of topographic breakthrough: The transmission

The intersection of the topography with the upper layer will now be shown to modify the transmission of the Kelvin wave, in contrast with the case of no topographic breakthrough. As in section 5, we write η and ϕ as (5.1), (5.2), together with

$$\psi(x, B) = \sum \alpha_n P_n(x)\exp(il_n B). \quad (8.1)$$

Substitution into (6.3), (6.4) gives two equations for $|\eta_T|$ as before. It is easily shown that orthogonality occurs, with appropriate replacement of some integrals by $C[\cdot]$, etc., just as in section 5; the algebra will not be given here. We thus have

$$\{s/(s+1)\}(\eta_T - 1) + C[(1 - D)v_B] = \{s/(s+1)\}(\eta_T - 1) + \sum \alpha_n C[F_n(D' - \omega l_n F_n)] = 0 \quad (8.2)$$

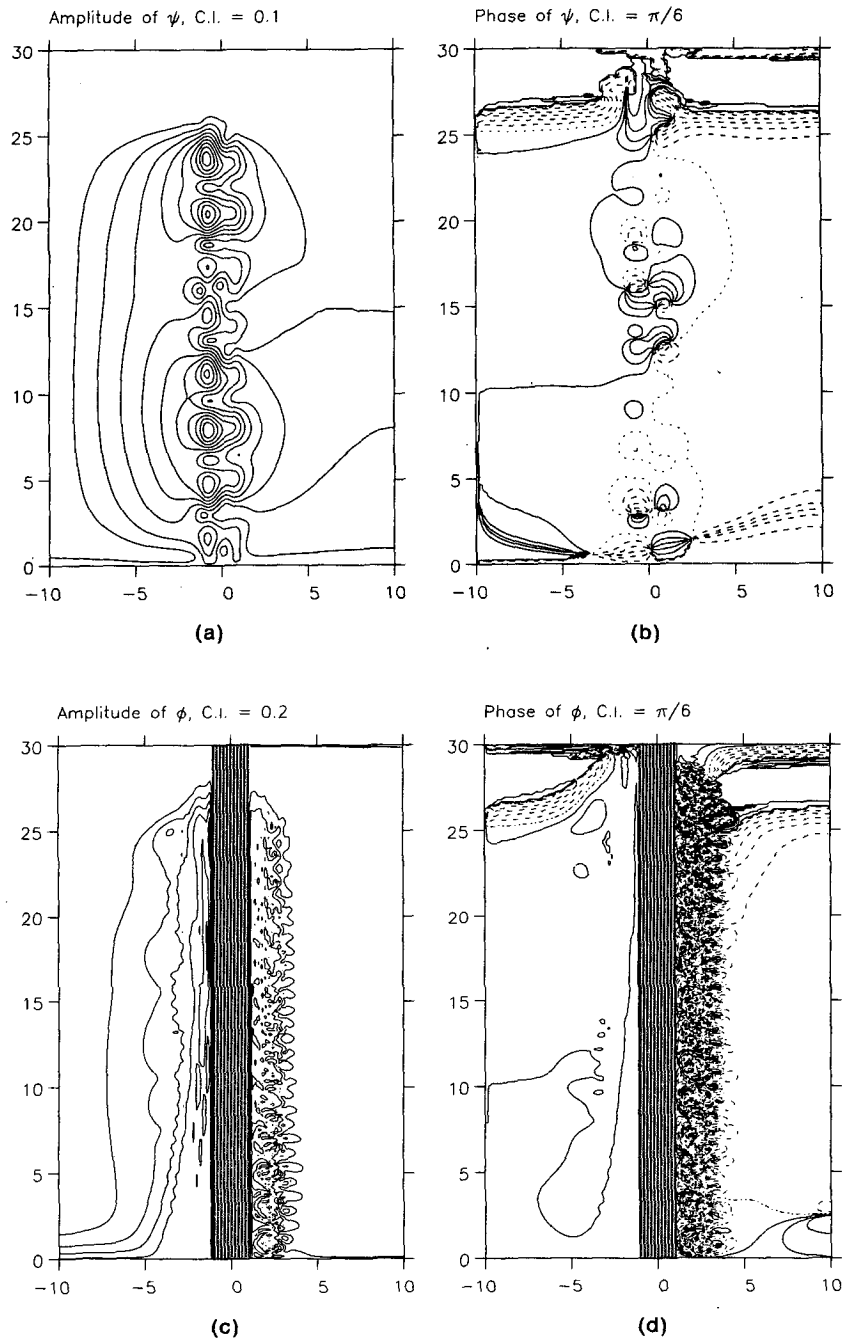

FIG. 9. An approximate numerical solution for topography (7.10), and $\omega = 0.02$. See Fig. 4 for details. The topographic breakthrough is indicated by cross-hatching where relevant. Note that this solution varies with resolution, box size, and linear damping, and should thus merely be regarded as indicative of the type of solution. The resolution (100×400) is not sufficiently good to give an accurate answer.

$$\{s/[2(s+1)]\}(|\eta_T|^2 - 1) + \sum |\alpha_n|^2 \left\{ \int dx(s - D_1)P_n(P_n' - \omega l_n P_n) + C[(1 - D)F_n(F_n' - \omega l_n F_n)] \right\} = 0. \quad (8.3)$$

It is straightforward to show that, as usual, the short waves give negligible contributions to both expressions. The terms, apparently $O(\omega)$ in (8.3), turn out to be so and can be neglected against what will shortly be shown to be $O(1)$ terms. However, numerical evaluation of the terms which are apparently $O(\omega)$ in (8.2)

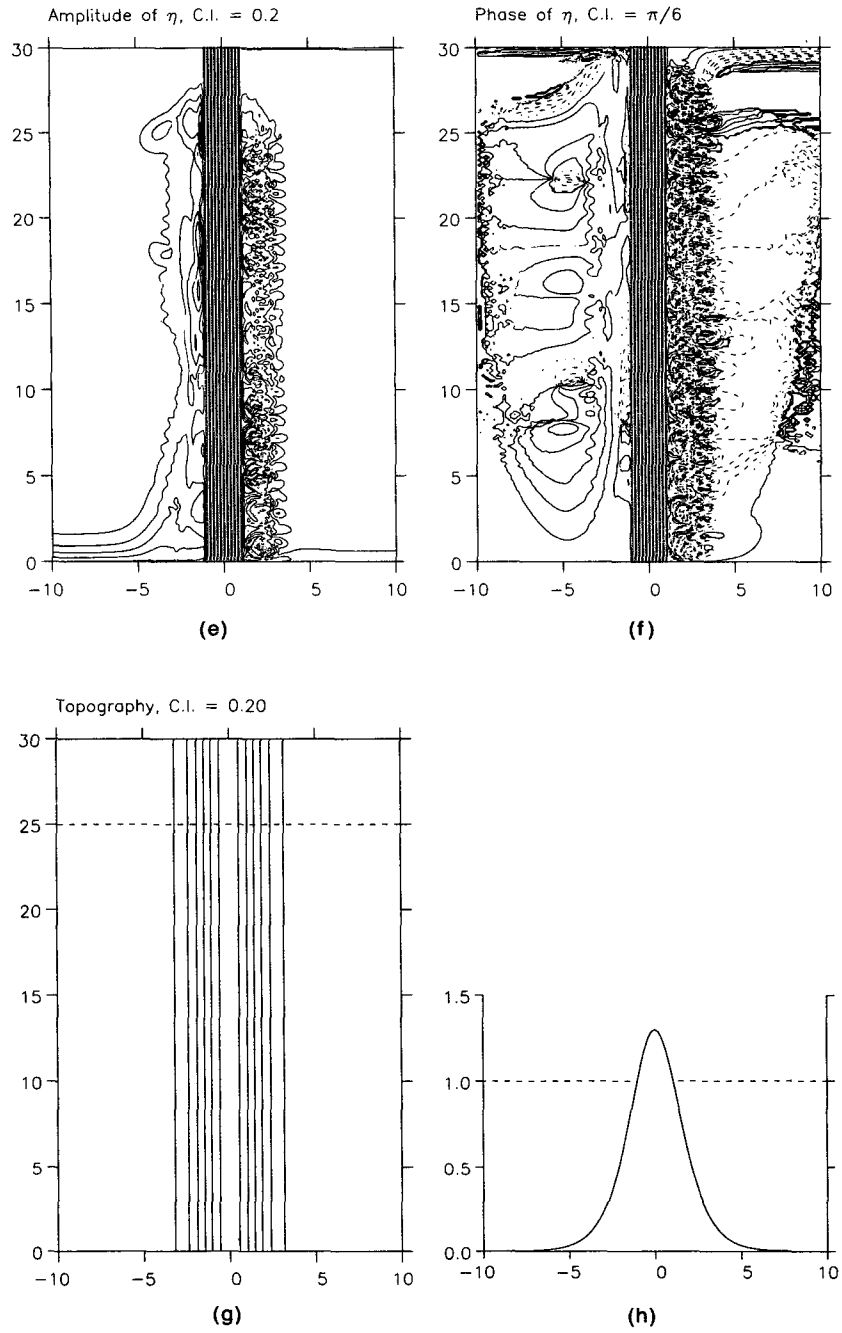

FIG. 9. (*Continued*)

is more complicated, as we saw in section 5, because of the slow decay at infinity. By using (6.4) to rewrite the expression in terms of the upper-layer pressure, (8.2) can be rewritten

$$\{s/(s+1)\}(\eta_T - 1) + \sum \alpha_n \left\{ \omega l_n s C[P_n] - \int D' P_n dx \right\} = 0. \quad (8.4)$$

Now the first term in the sum is truly $O(\omega)$ and can be neglected, while the second term is $O(1)$. Thus (8.4) simplifies to

$$\{s/(s+1)\}(\eta_T - 1) + \sum \alpha_n \left\{ -\int D' P_n dx \right\} = 0, \quad (8.5)$$

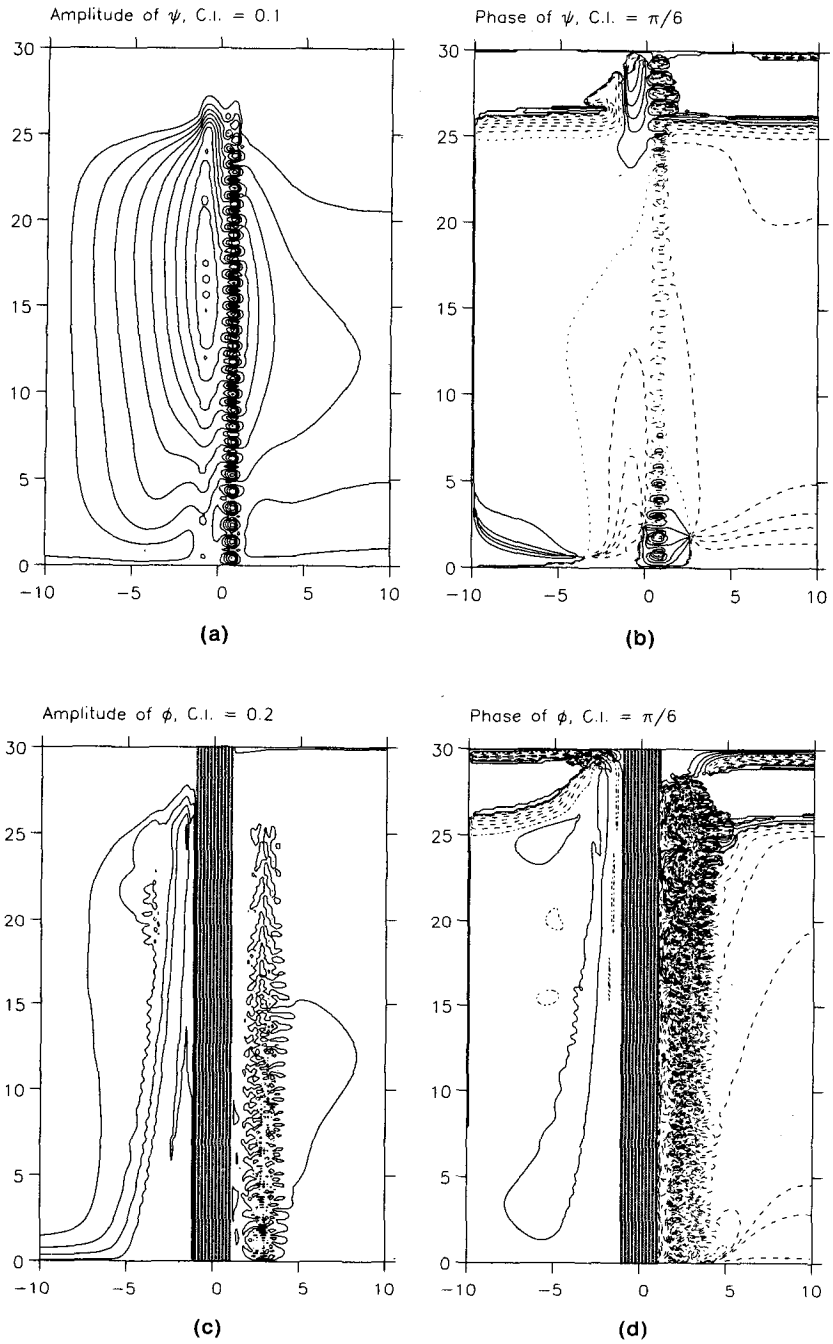

FIG. 10. As in Fig. 9, but for $\omega = 0.01$. The same comments about accuracy apply.

while (8.3), after removal of the $O(\omega)$ terms, gives after some integration by parts

$$\{s/(s+1)\}(|\eta_T|^2 - 1) + \sum |\alpha_n|^2 \left\{ \int D'P_n^2 dx + C[D'F_n^2] \right\} = 0. \quad (8.6)$$

If we now redefine

$$\gamma_n = -\int D'P_n dx \quad (8.7)$$

$$\mu_n \gamma_n^2 = \int D'P_n^2 dx + C[D'F_n^2] \quad (8.8)$$

then the algebraic problem reduces precisely to (5.10), (5.11), which have already been solved for $|\eta_T|$ in (5.14). It turns out numerically that the μ_n are positive for the long waves and the QB mode. The latter's μ_0 varies as ω^{-1} as in the case of no topographic breakthrough, but the long waves all have μ_n tending to constant nonzero values as $\omega \to 0$. Thus the formula (5.14)

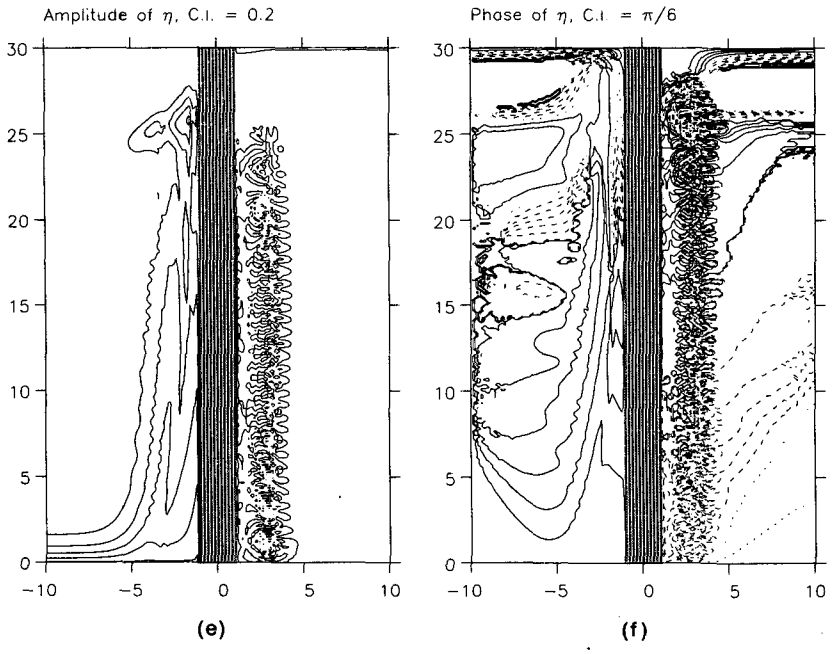

FIG. 10. (*Continued*)

predicts a finite energy loss by the Kelvin wave as it passes the topography.

The difference between this case and that of no breakthrough is fairly simple to understand. In both cases, the v field in the upper layer is predominantly geostrophic (for long waves). The integration of the mass flux along the topography involves a multiplication by the local upper-layer fluid depth. When there is no breakthrough, this depth is uniform, and the x-integral of the mass flux gives a cancellation to leading order through the geostrophic balance. Since there is no barotropic flow, there is no net mass flux along the topography in the lower layer either; hence the Kelvin wave continues at the same amplitude.

When there is breakthrough, however, the upper-layer fluid depth varies in the region (x_-, x_+), and the x-integral does not lead to total cancellation (just as in I, when there was only one layer). Then a finite amount of mass can be transported (oscillatorily) along the topography; these fluxes lead to the finite energy loss by the wave.

A numerical example gives an indication of this loss. Taking the case (7.10), we find that the first three long modes all have high μ (2615, 497, and 111, respectively, in the long wave limit). Most of the energy reduction is achieved by mode 4, with a μ of 12.4. Higher modes see rather higher μ's again: 63.4, 581, etc. (This is atypical: for higher topography, the first few modes are responsible for loss of transmission, as in I.) Substitution into (5.14) shows that the transmitted amplitude is at most 87%. The accuracy of the long-wave approximation can be gauged from the solution for $\omega = 0.01$, with μ of 2510, 510, 115, 11.1, 62.8, etc. (and a predicted maximum transmission of 87% again).

Two limits may be briefly noted. The first is $s \to \infty$, i.e., the upper layer becoming very deep. It is natural to expect that the limit would be that of the one-layer fluid considered in I. However, there are problems about interchanging the order in which limits are taken. Instead, letting s become large in (4.7), (4.8) and (7.9) and pursuing some simple algebra shows that the μ_n tend to infinity like s^2. The transmission formula (5.14) then demonstrates that there is no loss of energy, just as in the case of no breakthrough. (The reason is straightforward: the mass integral discussed above once more reduces approximately to an x-derivative and so cannot contribute to an energy loss.)

The second limit is when the topography approaches the upper boundary closely. Numerical solutions for the μ_n then show that, as expected, the transmitted energy approaches zero as the topography nears the upper boundary. In other words, the narrow gap through which fluid may pass acts as a rigid wall in the limit, and blocks all throughflow.

If the maximum topographic height $D_{\max}$ is permitted to vary in (7.10), a graph of transmission versus topographic height can be obtained (Fig. 8). For $D_{\max}$ less than 1, there is complete transmission since the topography does not break into the upper layer. The initial decay from 100% transmission is gradual, and then the dependence of transmission on $D_{\max}$ is roughly linear, as in I, except for a very rapid drop just before $D_{\max}$ reaches 5 (the depth of the upper layer, corresponding to complete blocking as mentioned above).

The rule of thumb thus remains that the transmitted amplitude roughly varies as the fractional depth above the highest point of the topography.

Attempts to confirm these results by direct numerical solution of the governing equations proved to stretch numerical resources to their limits. It has been impossible to show whether the predicted upper bound is attained, as in all previous calculations. Figures 9 and 10 show two numerical examples of such attempts, for the case (7.10), with $\omega = 0.02, 0.01$ respectively. The resolution in x and y was 0.2, 0.075 deformation radii, respectively. Although the phase variation of the solution on the upslope (negative x) is very gradual, since the waves are long, the rapid change in x for the solutions near the topographic breakthrough (shown in Fig. 5) makes it difficult to resolve the solution adequately. The short waves, for positive x, are still more difficult to resolve. The predicted transmissions are in error, and vary nonuniformly with resolution and frequency. There is also a strong dependence on box size, and the type of damping used at the northern boundary.

Many cases were run, varying box sizes, damping schemes, and damping coefficients. Computed transmissions for the interface displacement (which has no slow spatial decay terms like the two pressures, which tends to mask their true transmission values) varied from 13% to 145%, with most under 50%. It should be stressed that all solutions appeared visually plausible.

We are thus forced to conclude that it is impossible to resolve and reproduce correct numerical solutions for the two-layer breakthrough problem, even using a supercomputer. Thus, use of ocean general circulation models, whose resolution is far worse than used here, must inevitably lead to erroneous transmission of coastal waves within the models. (It was shown in I that the addition of dissipative terms did not alter this result, even though short waves, the poorest resolved, are filtered out.)

9. Discussion

This paper has considered the natural extension of Killworth (1988) to two active fluid layers. There are no formal reasons why this extension process cannot continue, to three, four, or many layers, and indeed it is clear that the formalism developed here will continue without difficulty. In fact, it is perfectly straightforward to pose the problem for a continuously stratified fluid, using density coordinates to mimic the layered model approach used here. Only a few details will be given here for brevity; the author can supply more information on request.

Almost all of the qualitative findings in this paper carry over to the continuous case. There are an infinite number of mass conservation equations, one for each density stratum, and a single energy conservation equation. There are again three types of topographic mode, many details of which have been explored by Huthnance (1978) for a continental slope topography. (For strong stratification, one can identify in this terminology the quasi-barotropic mode, long and short waves; the short waves are both bottom-trapped in the vertical and restricted in the horizontal dimension; as the stratification weakens, the distinction blurs.) Orthogonality of the modes continues in the energetic calculation.

The difference occurs because an infinite number of transmitted Kelvin wave modes is now possible (a similar feature occurs, plus backscattering, if one uses this formalism to examine scattering of shelf waves by topography). Thus the maximization/minimization arguments must now specify that one seeks an extremum of the transmitted amplitude of the mode specified as incoming. Of course, the result, even if calculable—very many topographic modes would have to be computed, each a lengthy calculation as Huthnance (1978) showed—could have less immediate use than the one- and two-layer calculations. This is because there does not appear any way to compute transmissions directly as a check on the calculations, so that it is not known whether the predicted upper bound serves as an accurate estimate of the actual transmission.

It now seems fairly clear, however, that the breakthrough of one or more density strata by topography plays a key role in governing wave transmission at low frequencies. Thus layered models which restrict topography to their lowest layer, and those with only small-amplitude topography, are likely to give erroneous answers in the regimes considered here. The same is true of most numerical models, which cannot adequately resolve the wide range of wave scales generated by the topography at low frequencies.

Acknowledgments. My thanks as ever to Jeff Blundell for programming the lengthy, and often contradictory, numerical studies that went into this paper, and for helpful suggestions on the text.

REFERENCES

Huthnance, J. M., 1978: On coastal trapped waves: Analysis and numerical calculation by inverse iteration. *J. Phys. Oceanogr.*, **8**, 74–92.

Johnson, E. R., 1989: The low-frequency scattering of Kelvin waves by stepped topography. *J. Fluid Mech.*, submitted.

Johnson, G. C., and H. L. Bryden, 1988: On the size of the Antarctic Circumpolar Current. *Deep-Sea Res.*, in press.

Killworth, P. D., 1988: How much of a coastal Kelvin wave gets over a ridge? *J. Phys. Oceanogr.*, in press.

Mysak, L. A., 1980: Topographically trapped waves. *Ann. Rev. Fluid Mech.*, **12**, 45–76.

Willmott, A. J., 1984: Forced double Kelvin waves in a stratified ocean. *J. Mar. Res.*, **42**, 319–358.